Powder Technology 275 (2015) 199–210

Contents lists available at ScienceDirect

Powder Technology

journal homepage: www.elsevier.com/locate/powtec

Emulsion phase expansion of Geldart a particles in bubbling fluidized bed methanation reactors: A CFD–DEM study

Yuli Zhang [a,b], Mao Ye [b], Yinfeng Zhao [b], Tong Gu [c], Rui Xiao [a], Zhongmin Liu [b,*]

[a] School of Energy and Environment, Southeast University, Nanjing 210096, China
[b] Dalian National Laboratory for Clean Energy, National Engineering Laboratory for MTO, Dalian Institute of Chemical Physics, Chinese Academy of Sciences, Dalian 116023, China
[c] BP Energy Innovation Laboratory, Dalian 116023, China

ARTICLE INFO

Article history:
Received 31 October 2014
Received in revised form 31 December 2014
Accepted 27 January 2015
Available online 31 January 2015

Keywords:
Fluidized bed
Methanation
CFD–DEM
Fluidization quality
High pressure

ABSTRACT

In fluidized bed methanation reactors, gas volumetric flow reduction due to the reaction can cause serious problems for fluidization quality, and in extreme cases, unwanted *defluidization* may occur. Note that the fluidization quality is closely linked to the expansion of emulsion phase, this paper present a numerical study on the emulsion phase expansion of Geldart A type of particles in fluidized bed methanation reactors by use of the well-established CFD–DEM model. The effects of operation conditions such as reaction rate, superficial gas velocity, pressure and bed inventory are discussed and compared qualitatively with experiments in literature. It is found that a higher gas velocity, based on the reactant gas at the inlet, is required to fully fluidize the particles and maintain good fluidization quality in a methanation reactor. Fast bubbles, considered as an important feature in the fluidization of Geldart A type of particles, were observed. Close check shows that the gas circulation around fast bubbles is responsible for the worsened gas exchange between gas bubbles and emulsion phase and consequently the apparent contraction of emulsion phase for Geldart A type of particles. Higher pressure and lower bed height can improve emulsion phase expansion in the methanation fluidized bed reactors, which is in accordance with previous experimental findings. The superficial gas velocity affects the emulsion phase expansion in a complicated way, where two mechanisms, i.e., large bubble size and short gas residence time, will work together.

1. Introduction

Fossil fuels such as oil, natural gas and coal have been used worldwide as energy resource for transportation and raw materials for chemical production. Despite the rapid rise of oil price and a surging demand for fossil fuels, the usage of coal and renewable biomass as a substitute energy resource is becoming increasingly important. One of the technologies attracting considerable interest nowadays is the transformation of synthesis gas, which is produced from either coal or biomass steam gasification, to synthetic natural gas (SNG). Coal or biomass to SNG has higher conversion and better heat efficiency, and can take advantages of existing pipeline and end-user market [1,2].

The SNG process involves typically two key steps: gasification and methanation. In the gasification step, synthesis gas containing mainly hydrogen and carbon monoxide is produced via a coal or biomass gasifier. Then in the consequent methanation step, hydrogen and carbon monoxide are transformed to methane through a catalytic hydrogenation process. In a methanation reactor, the following three reactions can take place simultaneously:

$$CO + 3H_2 \leftrightarrow CH_4 + H_2O \qquad (\Delta H_r^0 = -206 KJ/mol) \tag{1}$$

$$CO + H_2O \leftrightarrow CO_2 + H_2 \qquad (\Delta H_r^0 = -165 KJ/mol) \tag{2}$$

$$2CO \leftrightarrow CO_2 + C \qquad (\Delta H_r^0 = -173 KJ/mol) \tag{3}$$

The main reaction (1), i.e., the methanation reaction, transforms carbon monoxide and hydrogen to methane and water. The water gas shift reaction (2) is associated with the methanation reaction [2], and can change the ratio of hydrogen to carbon monoxide in the methanation reactor. The Boudouard reaction (3) also occurs together with the methanation reaction, but will raise risk of catalyst deactivation due to the deposition of coke on catalyst surface [3]. Note that all three reactions in the methanantion step are highly exothermic, the efficient removal of reaction heat from a methanation reactor is, therefore, extremely important to avoid local hot spots, prevent the catalyst from sintering, and achieve high carbon monoxide conversion and methane selectivity.

* Corresponding author.
E-mail addresses: maoye@dicp.ac.cn (M. Ye), zml@dicp.ac.cn (Z. Liu).

http://dx.doi.org/10.1016/j.powtec.2015.01.064
0032-5910/

Several SNG processes [4–8] have been developed since 1970s and some are commercially available today. In most of these SNG processes fix bed is adopted as methanation reactors. However the inherent temperature gradient in fixed bed requires high product gas recycle ratios, serial connection of multiple gas coolers, and low inlet H_2/CO ratio in order to remove the reaction heat and control temperature distribution in the reactors. These methods certainly add extra capital expenditure and increase the energy consumption. Compared to fixed bed reactors, fluidized bed reactors have been shown more suitable for heterogeneously catalytic reactions with strong exothermicity, owing to the great heat transfer performance and operational flexibility. Moreover, it was demonstrated that fluidized bed methanation reactors can help to reduce coke deposition on the particle surface [7,8].

Yet there are some challenges to be addressed in the development of industrial fluidized bed methanation reactors. For example, the fluidization of catalyst with a reduced gas volumetric flow in a highly exothermic environment has not been fully understood. In the carbon monoxide methanation reaction (1), the number of gas moles is changed from 4 to 2. This will lead to a significant reduction of gas volumetric flow in the emulsion phase since the methanation reaction mainly takes place in the emulsion phase. If the gas volumetric flow decreased in the emulsion phase cannot be compensated by the gas flow from the bubble phase, it will cause serious contraction of emulsion phase and, in extreme case, even partial *defluidization* [9,10]. Good fluidization quality is highly desired for the optimal and safe operation of fluidized bed methanation reactors.

The influence of gas volumetric flow change on fluidization quality in bubbling fluidized beds has been studied either experimentally or numerically by researchers. Kai and his co-workers [10–12] carried out a series of experiments of carbon dioxide methanation, and showed that a worsened fluidization quality in bubbling fluidized bed reactors with apparent contraction in the emulsion phase. They found that the declension of fluidization quality could eventually lead to the failure of reactor operation. Li and Guenther [13] investigated the influence of gas volumetric flow change caused by ozone decomposition reaction on the fluidized bed hydrodynamics based on 2D MFIX-DEM simulations. It was shown that the gas volumetric flow change affects the bubble characteristics to certain extend. Yet in their work, only Geldart B particles (size of 200–500 μm) were considered. Wu et al. [14] performed a CFD–DEM simulation for the synthetic gas methanation process in a fluidized bed reactor and observed unwanted *defluidization* phenomenon by altering the superficial gas velocity for Geldart B particles. However, Wu et al. [14] did not report any detailed information on the bubble behavior and emulsion phase contraction. Chu et al. [15] presented an interesting emulsion phase contraction model to predict the fluidization quality for varying reaction temperature and gas feed conditions. In their model, Chu et al. [15] assumed that the emulsion phase is a porous domain, and key parameters such as emulsion phase voidage and inter-phase mass transfer coefficients were obtained from empirical correlations. However, the use of traditional empirical correlations to predict emulsion phase voidage and mass transfer between the emulsion phase and bubble phase in fluidized bed methanantion reactors needs to be further validated. In a very recent contribution, Liu and Hinrichsen [16] used an Eulerian–Eulerian two-fluid model to simulate a fluidized bed methanation reactor. They also found a weak bed expansion due to the methanation reaction with gas volume reduction [16].

Practically Geldart A type of catalyst particles have been mostly in fluidized bed catalytic processes such as fluid catalytic cracking (FCC) and methanol to olefins (MTO), due to the good fluidity and high mass transfer efficiency. It was found in our previous study that the fluidization behavior of Geldart A particles is different from that of Geldart B particles with reduced volumetric flow [17]. For Geldart B type of particles, the volumetric flow reduction has a negligible influence on emulsion phase expansion. For Geldart A particles, however, a pronounced contraction of emulsion phase was identified [17]. Kai et al. showed in their experiments that the expansion of emulsion phase is closely associated with fluidization quality [10,12,18], which in turn affects the mass transfer and reactor performance. The goal of this study is to understand the mechanism underlying emulsion phase expansion of Geldart A type of particles in bubbling fluidized bed methanation reactors.

The detailed information of the change of local viodage in the emulsion phase, which is a particle-scale phenomenon, is hard to be measured [10–12]. Fortunately the CFD–DEM model, which has been widely used in the particle scale simulations, is considered as a promising learning tool for studying the detailed gas–solid interaction in fluidized beds [19]. In current work, the CFD–DEM modeling approach will be employed to study the emulsion phase expansion of Geldart A particles with volumetric flow reduction. The CFD–DEM code used in this work was originally developed by Prof. Hans Kuipers' group at Twente University (now with Eindhoven University of Technology) [19–21], and has been successfully applied to various applications [22,23]. This paper is organized as follows. First, a short compilation of the physical and kinetic equations in the CFD–DEM model is introduced, which is followed by an investigation and discussion of minimum fluidization velocity and bubble dynamics in the methanation process. Then the effects of various operating conditions on the emulsion phase expansion are studied. The results are qualitatively compared with some experiments reported in literature, and are further analyzed in order to understand the physics behind the emulsion phase expansion.

2. Mathematical models

The gas phase is described by the Navier–Stokes equations, and the particle phase is modeled by a soft-sphere discrete particle model [21,23]. The motion of each particle is tracked by solving Newton's second law. The numerical solution of the gas phase is in accordance with Kuipers et al. [24].

2.1. Gas phase

The gas phase is modeled by the volume-averaged Navier–Stokes equations. The mass conversation can be described as

$$\frac{\partial\left(\varepsilon_g\rho_g\right)}{\partial t}+\nabla\cdot\left(\varepsilon_g\rho_g u_g\right)=S_g. \tag{1}$$

Here ρ_g is the gas density, ε_g the local void fraction, $\vec{u}_g$ the gas velocity and S_g the mass source term due to the coke formation reaction. Momentum conservation is

$$\frac{\partial\left(\varepsilon_g\rho_g\vec{u}_g\right)}{\partial t}+\nabla\cdot\left(\varepsilon_g\rho_g\vec{u}_g\vec{u}_g\right)=-\varepsilon_g\nabla p+\nabla\cdot\overline{\overline{\tau_g}}+\varepsilon_g\rho_g\vec{g}-S_p+S_{cd} \tag{2}$$

where p is the gas phase pressure, τ_g the viscous stress tensor, $\vec{g}$ the gravitational acceleration, S_p the momentum source term due to inter-phase interaction and S_{cd} the momentum source term due to the coke formation reaction. S_p and S_{cd} are defined as

$$S_p=\frac{1}{V_{cell}}\sum_{p=0}^{N}3\pi\mu_g\varepsilon_g{}^2d_p\left(\vec{u}_g-\vec{u}_p\right)f\left(\varepsilon_g\right)\delta\left(\vec{x}-\vec{x}_p\right) \tag{3}$$

$$S_{cd}=S_g u_g \tag{4}$$

with β being the momentum transfer coefficient, V_{cell} the local volume of a computational cell and N the particle number in the computational cell. The δ-function ensures that the drag force acts as a point force at the

particle center. The gas species is considered as ideal gases, the mixture viscosity is computed based on kinetic theory as

$$\mu_g = \sum_i \frac{X_i \mu_i}{\sum_j X_i \phi_{ij}} \tag{5}$$

where

$$\phi_{ij} = \frac{\left[1 + \left(\frac{\mu_i}{\mu_j}\right)^{1/2} \left(\frac{M_{w,j}}{M_{w,i}}\right)^{1/4}\right]^2}{\left[8\left(1 + \frac{M_{w,i}}{M_{w,j}}\right)\right]^{1/2}} \tag{6}$$

M_w the molecular weight of species i, and X_i is the mole fraction of species i.

The transport equation for each gas species is

$$\frac{\partial\left(\varepsilon_g \rho_g Y_i\right)}{\partial t} + \nabla \cdot \left(\varepsilon_g \rho_g Y_i \vec{u}_g\right) = \nabla \cdot \left(\varepsilon_g \rho_g D \nabla Y_i\right) + S_i \tag{7}$$

where Y_i is the mass fraction of the gas species i, D the mass diffusivity, and S_i is the source terms due to reactions. The diffusion coefficient D, is computed as

$$D = \frac{1 - X_i}{\sum_{j, j \neq i} \left(X_j / D_{i,j}\right)} \tag{8}$$

$D_{i,j}$ define the binary diffusion of species i in each species j which is calculated using kinetic theory.

The energy conservation is described as

$$\frac{\partial\left(\varepsilon_g \rho_g H_g\right)}{\partial t} + \nabla \cdot \left(\varepsilon_g \rho_g H_g \vec{u}_g\right) = -\nabla \cdot \left(\varepsilon_g \vec{q}\right) + S_{hr} + S + S_r. \tag{9}$$

Here H_g repents the gas enthalpy, $\vec{q}$ the fluid heat flux, S_{hr} energy source term due to the carbon deposit reaction, and S and S_r are the source terms of heat transfer between the two phases and the homogeneous reaction heat, respectively. S_{hr} is defined as

$$S_{hr} = S_g H_g. \tag{10}$$

2.2. Particle phase

The motion of a single particle, p, is described by Newton's second law:

$$m_p \frac{d\vec{u}_p}{dt} = \vec{F}_{cont,\ p} - V_p \nabla p + m_p \vec{g} + \vec{F}_{drag,\ p} \tag{11}$$

$$I_p \Omega_p = I_p \frac{d\varpi_p}{dt} \vec{Tr}_p. \tag{12}$$

Here m_p is the mass of particle, V_p the volume of particle, $\vec{F}_{cont,\ p}$ the contact force acting on the particle, $\vec{F}_{drag,\ p}$ the drag force, $\vec{Tr}_p$ the torque, I_p the moment of inertia, Ω_p the rotational acceleration, and ϖ_p the rotational velocity. A drag model derived from lattice Boltzmann simulation was used to calculate the drag force between the gas and particles [25]:

$$\vec{F}_{drag,\ p} = 3\pi \mu_g \varepsilon_g^{\ 2} d_p \left(\vec{u}_g - \vec{u}_p\right) f(\varepsilon) \tag{13}$$

where ε is the local void fraction and $f(\varepsilon)$ is characterized by

$$f(\varepsilon) = \frac{10(1-\varepsilon)}{\varepsilon^3} + 0.7 \quad for\ \varepsilon < 0.6 \tag{14a}$$

$$f(\varepsilon) = \frac{1 + 3\sqrt{0.5(1-\varepsilon)} + (135/64)(1-\varepsilon)\ln(1-\varepsilon) + 17.14(1-\varepsilon)}{1 + 0.681(1-\varepsilon) - 8.48(1-\varepsilon)^2 + 8.16(1-\varepsilon)^3} \quad for\ \varepsilon > 0.6. \tag{14b}$$

The detailed interaction between particles and between particles and the wall is calculated by a simplified spring–dashpot model [21].

The heat balance is calculated as follows:

$$m_p C_p \frac{dT_p}{dt} = q_{cont,\ p} + q_{cv} + q_r + q_{rad}. \tag{15}$$

In this expression, $q_{cont,\ p}$, q_{cv}, q_r and q_{rad} represent the particle–particle heat transfer by conduction, the gas–particle heat transfer by convection, the reaction heat generated by chemical reaction, and the heat transfer by radiation, respectively. $q_{cont,\ p}$ is simply calculated by Eq. (16) [26,27]

$$q_{cont,\ p} = \sum_{i=0}^{n} 2 a_i k_s \left(T_i - T_p\right) \tag{16}$$

where n is the number of the particles contacting with particle p, a_i is the contact radius, and k_s is the particle thermal conductivity. The convective heat transfer is determined by

$$q_{cv} = h_{cv} \pi d_p^2 \left(T_g - T_p\right). \tag{17}$$

And the heat transfer coefficient h_{cv} is calculated according to the Ranz correlation [28], which is given as follows:

$$Nu = \frac{h_{cv} d_p}{k_g} = 2.0 + 0.6 Re^{1/2} Pr^{1/3}. \tag{18}$$

Since the operating temperature in the methanation reaction is approximately 600 K, the radiation heat transfer is very small and will not be considered. Accordingly, S in Eq. (9) is characterized as

$$S = \frac{1}{V_{cell}} \sum_{p=0}^{N} q_{cv,i}. \tag{19}$$

The DEM time step should be smaller than the duration of the particle–particle contact to assure a stable calculation. In the linear spring–dashpot model, the oscillating period of a spring–dashpot system is $\tau = 2\pi\sqrt{m_e/k_n}$ [29]. It was found that dividing the oscillating period by a factor 10 can yield a stable simulation [30], and therefore the maximum time step for the DEM simulation using linear spring–dashpot contact model is 0.1τ. In this work, a maximum DEM time step of 6.2×10^{-6} s could be obtained when a spring stiffness of 7 N/m is chosen. In the simulations reported in this paper, the DEM time step is set as 5.0×10^{-6} s, and the CFD time step is 10 times the DEM time step.

2.3. Reaction kinetics

The methanation reaction rate is described by a Langmuir–Hinshelwood expression:

$$r = \frac{k K_c p_{CO}^{0.5} p_{H_2}^{0.5}}{\left(1 + K_c p_{CO}^{0.5} + K_{OH} p_{H_2O} p_{H_2}^{-0.5}\right)^2} \tag{20}$$

where the kinetic parameters are taken from literature [31]. The source term S_i in Eq. (7) is defined as

$$S_i = \alpha\varepsilon_g\left(1-\varepsilon_g\right)r\rho_P M_i. \quad (21)$$

Here M_i is the molar mass of each gas component i, ρ_P is the particle density, and α is a constant (1 for CH_4 and H_2O, −1 for CO, and −3 for H_2). Similarly q_r in Eq. (15) is given by

$$q_r = rm_p H_r \Delta t \quad (22)$$

where H_r is the heat of the catalytic reaction and Δt is the time step of the simulation.

3. Simulation setup

To achieve computational efficiency, a lab-scale rectangular 2-D dense fluidized bed was utilized in this work. Unless otherwise stated, the fluidized bed studied was 0.06 m wide and 0.24 m high. The motion of gas and particle in the thickness direction was not solved. The thickness of the bed was assumed to be the diameter of a single particle to improve the solid fraction prediction in the emulsion phase. Li and Guenther [13] proposed a method to calculate the solid volume fraction in the CFD–DEM simulation:

$$\varepsilon_p = 1.075\varepsilon_{p,2D} \quad (23)$$

where $\varepsilon_{p,2D}$ is the solid volume fraction in the fluidized bed of one-particle-diameter depth, and ε_p is the solid volume fraction applied in the conservation equations. Eq. (23) is used to calculate the solid volume fraction in this work. Geldart A particles considered here have a particle density of 1300 kg/m^3 and diameter of 100 μm. The computational domain was discretized at a uniform grid of 0.5 mm, i.e., 5 times the diameter of a single particle. Table 1 shows the simulation conditions and physical properties of the particles. Gas density was calculated using the ideal gas equation of state.

In reality, the non-uniformity of temperature in the reactor might lead to a change of the gas volumetric flow. As the current study focused on the influence of gas volume reduction caused by the reaction, the operating temperature was assumed to be a constant. It should be stressed that the temperature difference in the reactor is normally small because of good heat transfer performance of fluidized bed reactors. Therefore, the assumption of constant temperature can be justified. Practically there are many ways that can be used to remove the heat of reaction from the reactor. For example, the catalyst cooler and the inner heat coil. The way of heat remove is a subject of future publication.

The methanation reaction kinetics adopted in this paper was a Langmuir–Hinshelwood rate expression. Note that the methanation catalyst used by Kopyscinski et al. [31] was quite active and the reactants could be completely converted several millimeters above the gas distributor. In a traditional fixed bed methanation reactor, high product gas recycle loops are usually used for temperature control, resulting in a very low reactant concentration of the inlet fresh gas. For this reason, the catalyst used in a fixed bed must be sufficiently active to ensure high reactant conversion. It should be noted that catalyst with high activity is not appropriate for a fluidized bed methanation reactor because the gas at the inlet normally has a high reactant concentration, and if it contacts with the highly active catalyst the reaction might occur rapidly and cause temperature runaway as well as severe coke formation. Therefore, in our simulations the reaction rate expression was scaled by a factor, b, of about 0.0–0.1 to reduce the activity of the catalyst. The source term in Eq. (21) is hence reformulated as

$$S_{i,m} = b\alpha\varepsilon_g\left(1-\varepsilon_g\right)r\rho_P M_i. \quad (24)$$

There is no methanation reaction occurring when b goes to zero. Note that the catalyst shows a high selectivity to CH_4, and the CO_2 concentration in the product gas is relative low compared to that of CH_4, so we switched off the water gas shift reaction in the simulations reported in this paper, though the water shift reaction was incorporated into the CFD–DEM code.

Table 1
Parameters used in the simulations.

Parameters	Value
Particle number, [−]	300,000/480,000/600,000
Particle diameter, [μm]	100
Particle density, [kg/m3]	1300
Normal spring stiffness, [N/m]	7
Tangential spring stiffness, [N/m]	2
CFD time step, [s]	0.00005
Particle dynamic time step, [s]	0.000005
CO concentration at inlet, [wt%]	0. 7
H_2 concentration at inlet, [wt%]	0. 2
CH_4 concentration at inlet, [wt%]	0
H_{2O} concentration at inlet, [wt%]	0.01
CO_2 concentration at inlet, [wt%]	0.09

4. Results and discussion

4.1. Minimum fluidization velocity

Minimum fluidization velocity is critical in methanation reactor operations, as the volumetric flow reduction might cause a change of the gas velocity along the bed height direction. The *measured* pressure drop in the simulations, as a function of the inlet superficial gas velocity, is plotted in Fig. 1. Here the minimum fluidization velocity U_{mf} is defined as the inlet superficial gas velocity at the point when the pressure drop just balances the weight of the fluidized catalyst inside the bed. As shown in Fig. 1, U_{mf} of about 0.00366 m/s can be *measured* for the case without the methanation reaction. Note that the inlet gas (see Table 1) has a density of about 0.16018 kg/m^3 and viscosity of 2.2626×10^{-5} Pa·s at a temperature of 600 K. The minimum fluidization velocity predicted based on the Wen–Yu correlation [32] under the same operating conditions is 0.0034 m/s. The predicted value of U_{mf} by the Wen–Yu correlation is about 93% of the *measured* value in our simulations.

When the methanation reaction is switched on, the inlet superficial gas velocity increases to 0.0053 m/s at the minimum fluidization point. This is because the superficial gas velocity will decrease along the bed height when the reactant gas contacts with the catalyst particles, as

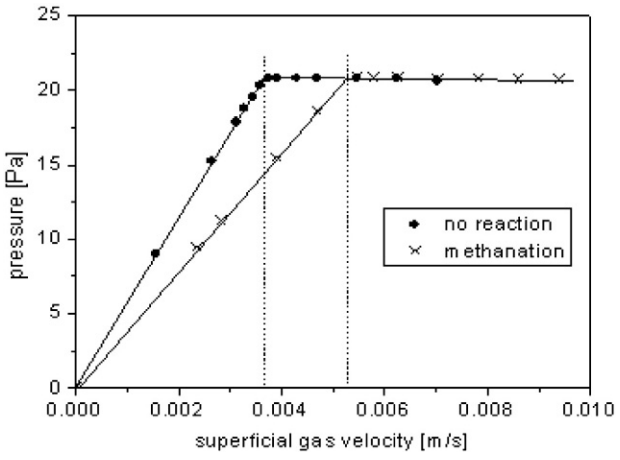

Fig. 1. Pressure drop across the methanation fluidized bed reactor as a function of the inlet superficial gas velocity. Simulations carried out in a 0.06 m × 0.24 m (W × H) fluidized bed under the conditions listed in Table 1.

can be seen in Fig. 2. In this case, a higher inlet gas velocity is needed to fully fluidize the catalyst particles in the bed. Fig. 2 also shows the time-averaged superficial gas velocity and cross-sectional averaged voidage along the bed height. In the dense bed regime, the superficial gas velocity decreases gradually from 0.0053 m/s to 0.00323 m/s along the bed height, as shown in Fig. 2b. In the upper part of the dense bed, CO is 100% converted and the product gas has a density of 0.2627 kg/m^3 and a viscosity of 2.2619×10^{-5} Pa·s. We calculated a minimum fluidization velocity of about 0.003413 m/s based on the Wen–Yu correlation, which is very close to the *measured* superficial gas velocity at the upper part of the dense bed in our simulation. The U_{mf} estimated based on the reactant gas at the inlet is much higher than that based on the product gas at the outlet. A close check with the mass fraction distribution of gas species at the minimum fluidized state in the methanation reactor, as shown in Fig. 3, suggests that the quick conversion of CO and H_2 in the regime near the gas distributor is responsible for the rapid reduction of the gas volumetric flow.

The local *defluidization* was identified by both experimental [11,33] and simulation study [14]. Some simulations were specifically carried out to illustrate the local *defluidization* in the bed. The results indicates that, when an inlet superficial gas velocity is relatively lower but still higher than the minimum fluidization velocity, the upper part of the bed is still closely packed while there is an apparent bed expansion near the gas distributor. Clearly the regime far from the gas distributor will be *defluidized* when the inlet superficial gas velocity is not high enough, due to the rapid reduction of the volumetric flow near the gas distributor. We argue that, in the practical design of a fluidized bed methanation reactor, one should be very careful in calculating the minimum fluidization velocity. It is recommended that the minimum fluidization velocity based on the product gas under the outlet conditions should be used in the methanation reactor design.

4.2. Dynamics of gas bubbles

Fig. 4 shows the typical transient bubbling flow patterns after a physical time of 20 s when the simulations reach a quasi-steady-state. Apparent bed contraction can be observed when the methanation reaction is turned on. The bed contraction reveals a reduction of the gas volumetric flow caused by the occurrence of methanation in the fluidized bed reactor. In their experimental investigations, Kai et al. [10–12] detected enlarged bubble size in the presence of carbon dioxide

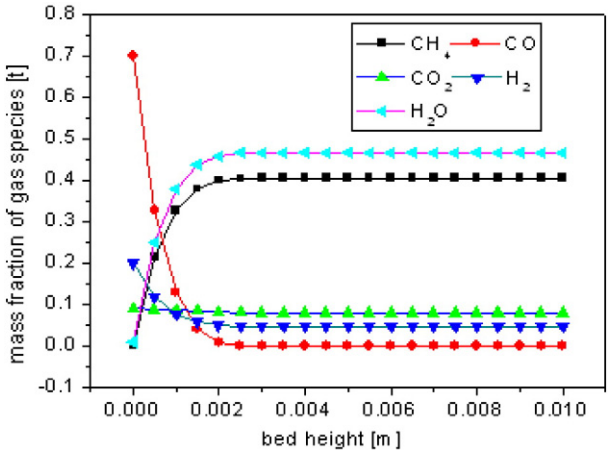

Fig. 3. Time-averaged mass fraction of the gas species along the bed height at the minimum fluidization point. Simulations carried out in a 0.06 m × 0.24 m (W × H) fluidized bed under the conditions listed in Table 1.

methanation reaction. In fact a close check with the simulation results at inlet superficial gas velocity of 0.05 m/s reflects that the maximum bubble size has been increased from 2.3 to 2.7 cm when the reaction coefficient *b* changes from 0 to 0.1. Here the region where the voidage larger than 0.55 is defined as gas bubbles, which otherwise are considered as the emulsion phase.

The presence of fast bubbles has been considered as one of the most important features of the fluidization of Geldart A type of particles [34]. Essentially the circulation of gas flow will be established around the fast bubbles. Fig. 5 shows the velocity field of gas near typical bubbles, in which the gas circulation can be clearly distinguished no matter the methanation reaction is turned on or not. Interestingly, such gas circulation patterns also exist in the enlarged bubbles as shown in Fig. 5(a) and (b). These enlarged bubbles are likely formed by coalesces of small bubbles nearby. In the enlarged bubbles the gas circulation patterns become more complicated with several vortexes developed. The gas circulations around fast bubbles make fresh reactants readily bypass through the dense bed, and weaken the mass transfer between gas bubbles and emulsion phase. It was suggested that in the presence of fast bubbles the mass transfer between gas bubbles and emulsion phase

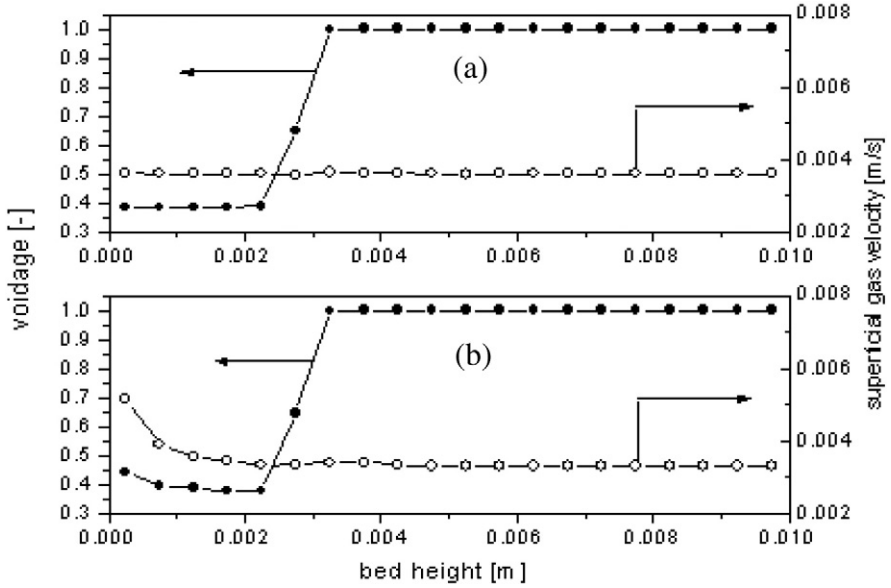

Fig. 2. Time-averaged superficial gas velocity and cross-sectional voidage along the bed height at the minimum fluidization point: (a) no reaction; (b) methanation reaction. Simulations carried out in a 0.06 m × 0.24 m (W × H) fluidized bed under the conditions listed in Table 1.

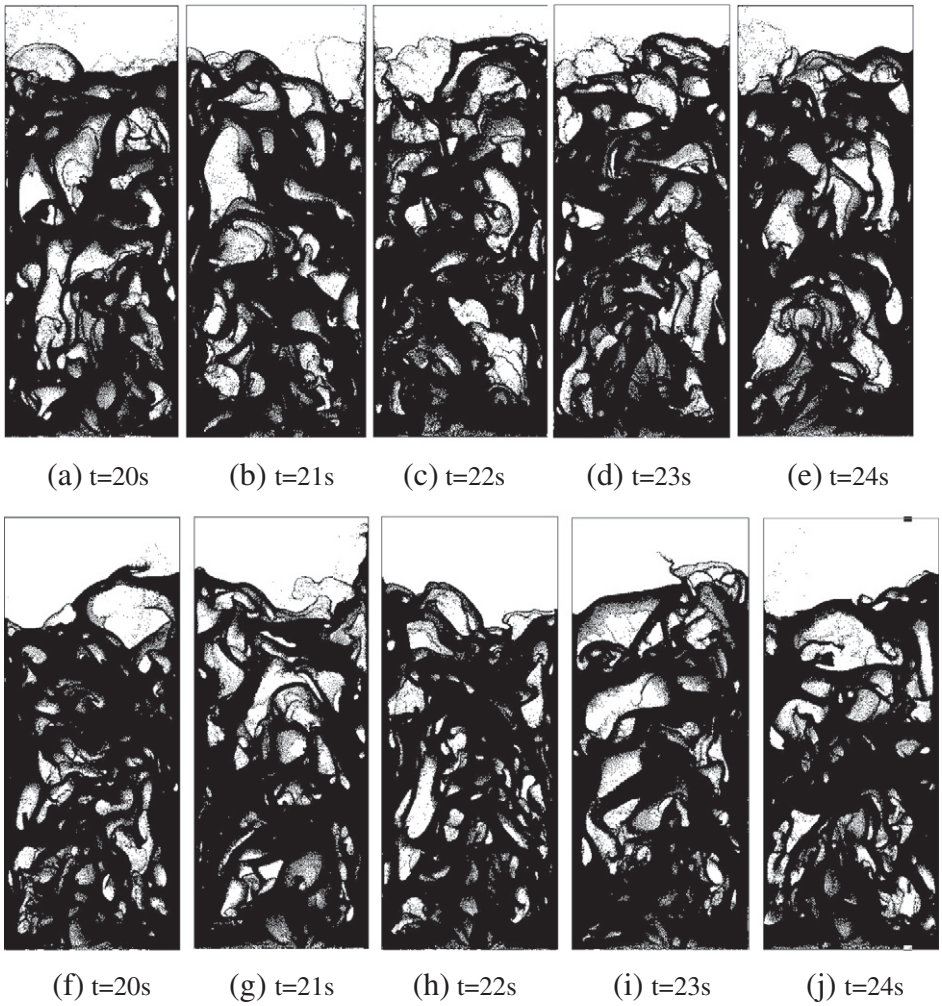

Fig. 4. Snapshots of bubbling flow patterns in a methanation fluidized bed reactor (W × H: 0.06 m × 0.24 m) at different physical time: (a–e) no reaction; (f–j) methanation reaction. Simulations carried out with a reaction coefficient *b* of 0.10, particle number of 480,000, pressure of 1 bar, and inlet gas superficial velocity of 0.10 m/s. Other simulation conditions listed in Table 1.

was mainly determined by throughflow velocity, bubble coalescence/split, and gas diffusion [34]. This can be evidenced from Fig. 6 where reactant-rich (CO/H_2) bubbles are found even at the top of the dense bed. Fig. 6 also shows the instantaneous mass fraction distribution of gas species (CO, H_2, H_2O, and CH_4), as well as the methane formation rate in the methanation reactor. It can be seen that the mass fractions of H_2 and CO in the emulsion phase decrease gradually along the bed height while CH_4 and H_2O show the opposite trends. The significant difference of gas compositions in the bubbles and emulsion phase suggests a limited interphase mass transfer in the dense bed.

4.3. Expansion of emulsion phase

To avoid hot spots and achieve high conversion, good fluidization quality is desired in a fluidized bed methanation reactor in order to maintain stable operations. Note that the methanation reaction mostly proceeds in the emulsion phase, the decrease of gas volumetric flow hence mainly occurs in the emulsion phase. In real operations, different methods should be taken to minimize the influence of the reduction of the gas volumetric flow and to improve fluidization quality. In carbon dioxide methanation experiments, Kai et al. [35] proposed measures such as product gas recycles, staged gas feed and baffled beds to improve fluidization quality.

Based on the previous analysis, the fluidization quality will become worse when there is a serve contraction of the emulsion phase. Therefore, the expansion ratio of the emulsion phase was used to indicate the fluidity of catalyst [36], rather than direct observation of *defluidization* in the bed. The voidage of the emulsion phase, ε_e, was calculated by taking the average over all computational cells in which the voidage is smaller than 0.55 and the mean voidage of the emulsion phase, $\overline{\varepsilon_e}$, is time-averaged for a certain time interval. The degree of expansion of the emulsion phase is characterized by the expansion ratio of the emulsion phase, δ_e, which is defined as

$$\delta_e = \frac{\overline{\varepsilon_e} - \varepsilon_{mf}}{\varepsilon_{mf}} \tag{25}$$

where ε_{mf} corresponds to the voidage of the dense phase at the minimum fluidization point, which is taken as 0.37 in our simulations. Note that when $\overline{\varepsilon_e}$ is in the range of 0.37–0.55, the expansion ratio of the emulsion phase should vary from 0 to 0.486.

4.3.1. Effect of the reaction rate

Fig. 7 depicts the time-averaged frequency distribution of the emulsion phase voidage. In one extreme where there is no methanation reaction ($b = 0$), the inlet superficial gas velocity shows a minor impact on the expansion of the emulsion phase. In another extreme when the

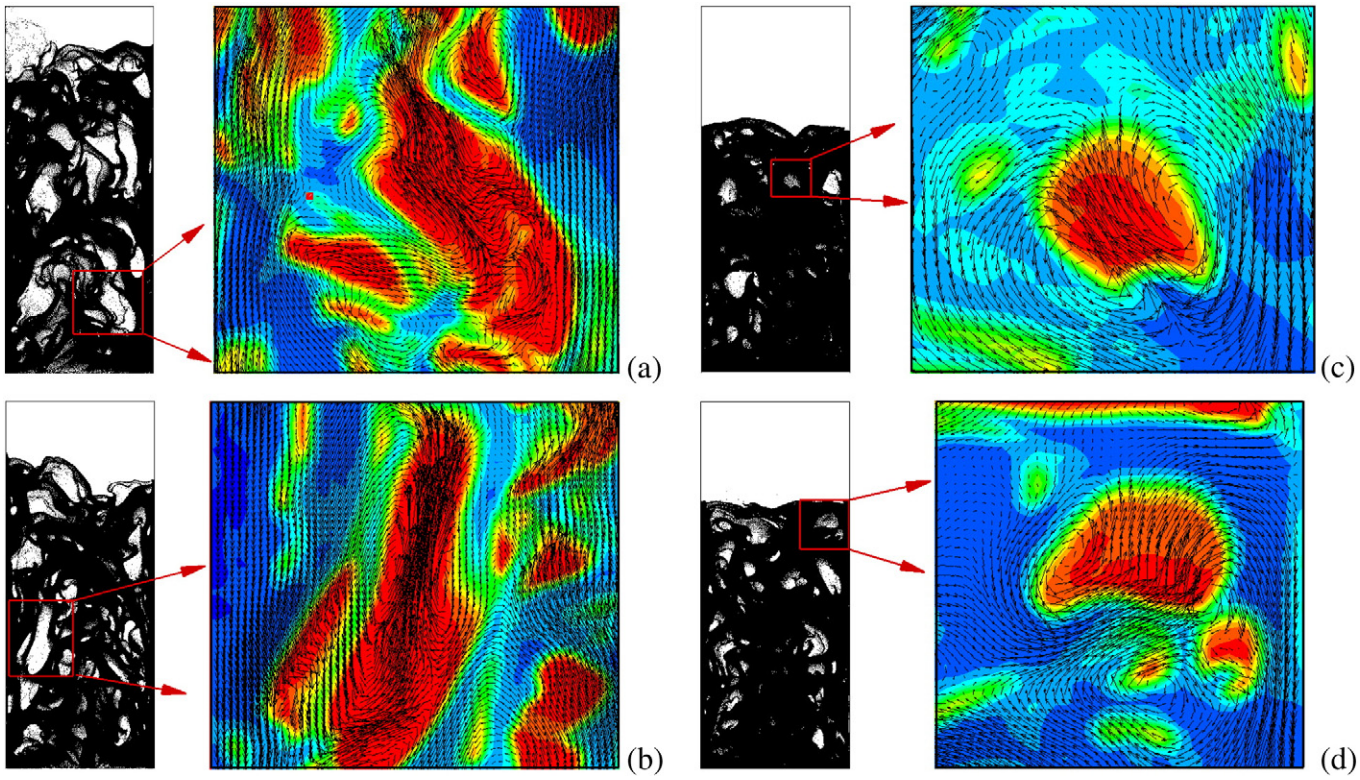

Fig. 5. Gas circulation around the gas bubbles in a methanation fluidized bed reactor (W × H: 0.06 m × 0.24 m). Simulations carried out with a reaction coefficient $b = 0$ for (a) and (c) and $b = 0.1$ for (b) and (d), particle number of 480,000, pressure of 1 bar, and inlet gas superficial velocity of 0.10 m/s for (a) and (b) and 0.05 m/s for (c) and (d). Other simulation conditions listed in Table 1.

reaction coefficient b goes to infinity, the reaction proceeds extremely fast and the reactants will be consumed very close to the gas distributor. In this case, the gas volumetric flow is significantly reduced near the gas distributor. Normally the reaction coefficient b is finite, and thus the mass transfer between the bubble and emulsion phase plays an essential role in the expansion of emulsion phase. Fig. 7 shows the simulation results with a limited reaction coefficient $b = 0.1$, where the peak of the emulsion phase voidage distribution shifts to lower values, compared to the situations with $b = 0$. This suggests that there is a contraction of the emulsion phase. Note that the expansion of the emulsion phase is usually considered as an important indicator closely linked to fluidization quality [10], the contraction of emulsion phase means a worsened fluidisation quality in the fluidized bed of Geldart A type of particles. As shown above, gas circulation around the fast bubbles will weaken the exchange of gas between gas bubbles and emulsion phase, thus the gas flow reduced in the emulsion phase cannot be completely replenished by the gas from the surrounding bubbles. This may explain the reason why a severe contraction of emulsion phase can be observed for Geldart A but not for Geldart B type of particles in presence of methanation reaction [17]. For Geldart B type of particles, slow bubbles with enhanced throughflow velocities will improve the mass transfer between gas bubbles and emulsion phase. The contraction of the emulsion phase will increase the effective viscosity of the emulsion phase, which consequently increases the shear resistance of the emulsion phase and weakens the catalyst mobility. This in turn makes the fluidization quality worse and thereby has a negative impact on the solid mixing rate as well as the heat transfer [37]. In extreme cases where gas velocity becomes very low and the drag force acting on the catalyst particles cannot balance the gravity, local *defluidization* may take place.

4.3.2. Effect of superficial gas velocity

Superficial gas velocity has a significant effect on fluidized bed operations [38]. Fig. 8 shows the expansion ratios of the emulsion phase under different inlet superficial gas velocities. In simulations where the methanation reaction is turned off ($b = 0$), an average voidage of the emulsion phase of 0.465 is found for an inlet superficial gas velocity of 0.025 m/s, and 0.464 for 0.15 m/s. This indicates that the inlet superficial gas velocity has a minor impact on the expansion ratio of the emulsion phase, which is in accordance with the experimental results by Kai et al. [39].

Fig. 8 also shows the expansion ratio of the emulsion phase at different inlet superficial gas velocities when the methanation reaction is turned on ($b = 0.05$). A non-monotonous change of the expansion ratio of the emulsion phase was found with an increasing superficial gas velocity. At a higher inlet superficial gas velocity, the bubble size becomes larger and the bed expansion shows an apparent increase. According to Chavarie and Grace [40], larger bubble size will reduce mass transfer between the bubble and emulsion phase, which thereby inhibits the gas from bubbles to compensate for the reduced gas volumetric flow in the emulsion phase, and lowers the fluidization quality in the fluidized bed reactor. In addition, the rising velocities of fast bubbles will increase at a higher inlet superficial gas velocity, resulting in a shorter gas residence time and a considerable gas bypass [41–43]. Higher reactant gas partial pressure can be found even at the top of the bed (see in Fig. 9). This means that less synthesis gas was converted, and the reduction of the superficial gas velocity in the emulsion phase thus becomes less serve, as illustrated in Fig. 10. The fluidization quality at a higher superficial gas velocity is actually dominated by the influence of the large bubble size and short gas residence time. These two mechanisms work together and result in the expansion of the emulsion phase changing in a complicated way.

Note that at higher inlet superficial gas velocities, the heat transfer in the bed can be enhanced due to vigorous solid mixing. It is therefore argued that a higher superficial gas velocity is more appropriate for operating a fluidized bed methanation reactor. This is especially beneficial in avoiding temperature runway [44].

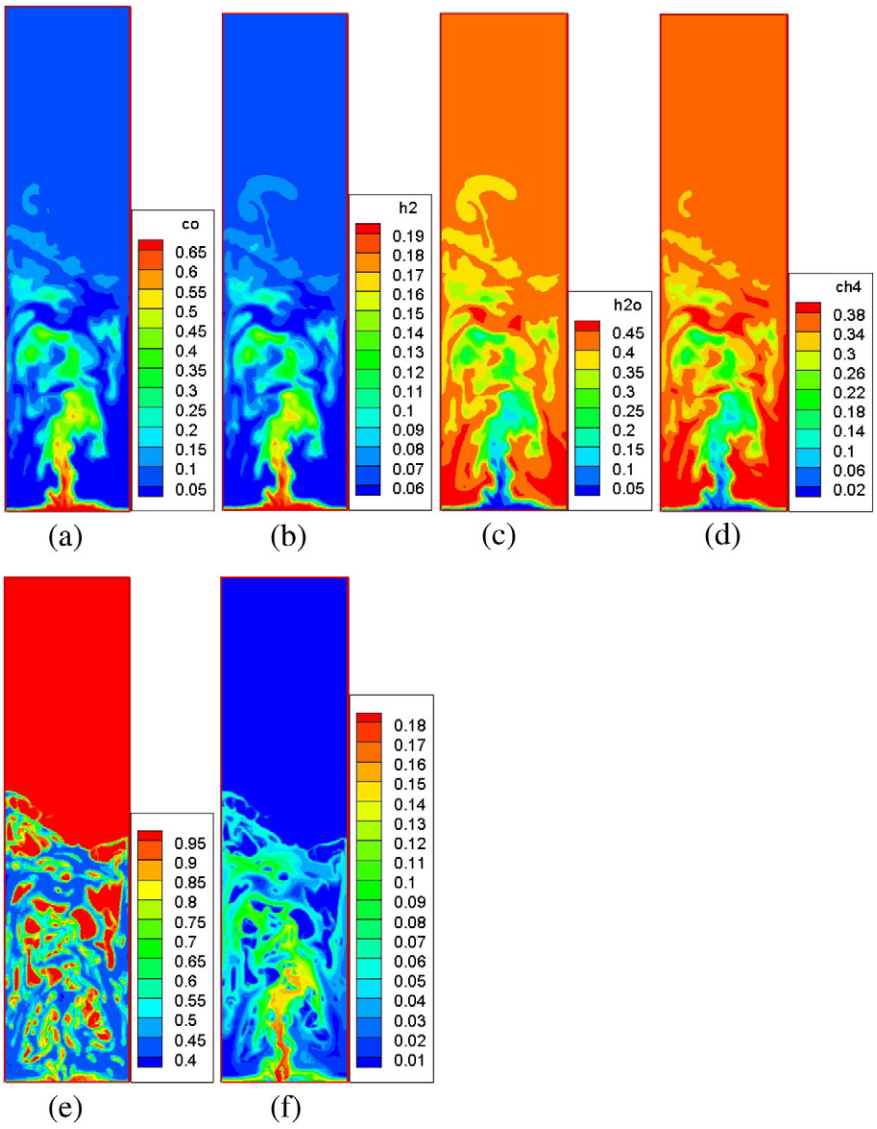

Fig. 6. The mass fraction distribution for gas species CO (a), H_2 (b), H_2O (c), CH_4 (d), the voidage distribution (e), and the methane formation rate ($kg \cdot m^{-3} s^{-1}$) (f) at the same moment in a methanation fluidized bed reactor. The simulation conditions listed in Table 1.

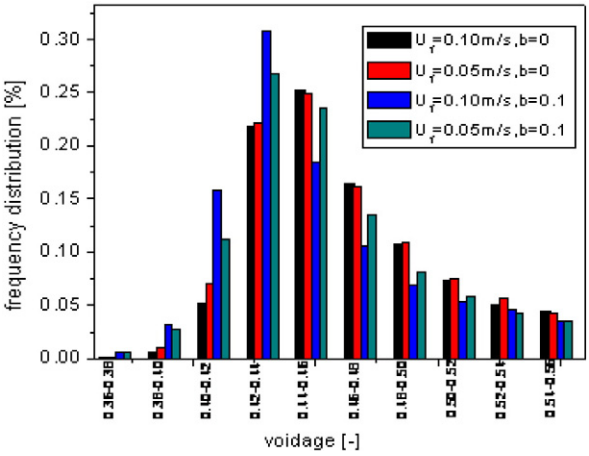

Fig. 7. Distribution of the voidage of the emulsion phase in a methanation fluidized bed reactor (W × H: 0.06 m × 0.24 m). Results are taken from the simulation at 20 s. Simulations carried out with particle number of 480,000 and pressure of 1 bar. Other simulation conditions listed in Table 1.

4.3.3. Effect of pressure

The methanation reaction results in a net decrease in the number of moles of the product gas, and hence it is favored at a higher pressures [45]. Moreover, high operational pressure means higher conversion and thus a reduction in the cost of the pipeline gas compression [46]. It is widely reported that pressure has a strong influence on the hydrodynamics of a fluidized bed [47], therefore it is important to understand the effect of pressure on the emulsion phase expansion in fluidized bed methanation reactor.

Fig. 11 shows the flow patterns and corresponding distributions of methane formation rate ($kg \cdot m^{-3} s^{-1}$) in the methanation fluidized bed reactor at 20 s, and Fig. 12 shows the dependence of the expansion ratio of the emulsion phase on operating pressure at a constant inlet superficial gas velocity of 0.1 m/s. At a lower operating pressure, the reaction has an apparent impact on the expansion ratio of the emulsion phase. The *measured* expansion ratio of the emulsion phase declines from 0.251 to 0.216 at an operating pressure of 1 bar when the methanation reaction is turned on, which accounts for roughly 14.0% of the emulsion phase. At a higher pressure of 40 bar, when the reaction is considered, the *measured* expansion ratio of the emulsion phase

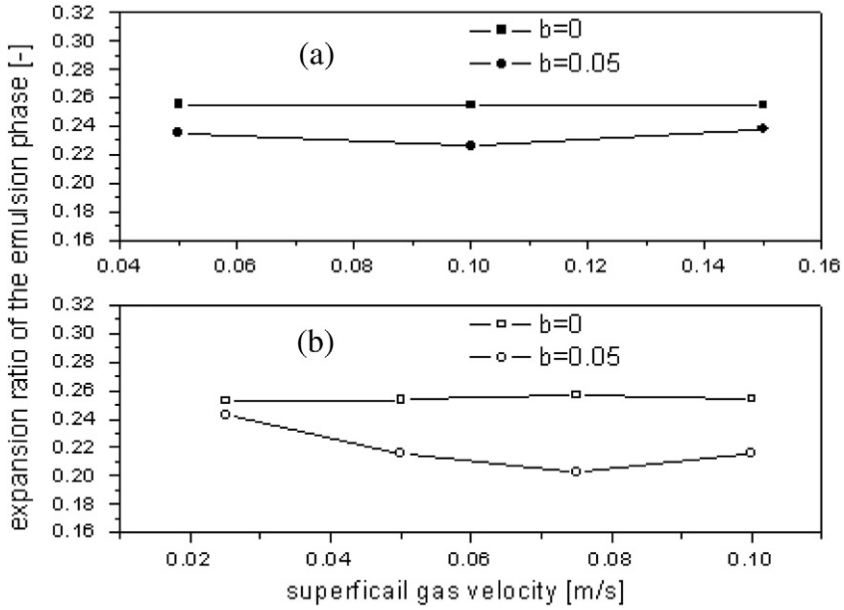

Fig. 8. Effect of inlet superficial gas velocity on the expansion ratio of the emulsion phase in the fluidized bed methanation reactor (W × H: 0.06 m × 0.24 m). Simulations carried out with particle number of 300,000 for (a) and 480,000 for (b), temperature of 600 K, and pressure of 1 bar. Other simulation conditions listed in Table 1.

declines from 0.303 to 0.289, which is only 4.5%. As shown in Fig. 12, the higher the operating pressure, the higher the expansion ratio of the emulsion phase. In fact, the expansion ratio of the emulsion phase depends on the properties of the fluidizing gas [18], and increases with an increasing gas density and/or viscosity. Pressure has a negligible effect on the gas viscosity (and is assumed constant in our simulations) but can lead to a substantial increase in gas density, bringing about an apparent expansion of the emulsion phase. The increased pressure will favor bubbles splitting into small voids [48,49], prompt the throughflow velocity [50], and improve mass transfer between gas bubbles and emulsion phase. Fig. 6(e) and Fig. 11(a) show the flow patterns at two different pressures. It can be seen that there is an apparent reduction in bubble size when the pressure increases from 1 bar to 40 bar. From Fig. 6(d) and Fig. 11(b), it can be anticipated that the difference of CH_4 mass fraction distribution between the two phases becomes smaller at a higher pressure, indicating the decrease in bubble size will lessen the mass transfer resistance between the bubble phase and the emulsion phase [40]. Therefore, the gas flow consumed in the emulsion phase can be easily compensated by the gas from the bubbles at elevated pressures. Nevertheless, higher operating pressure improves the emulsion phase expansion, and thus improves fluidization quality in a methanation fluidized bed.

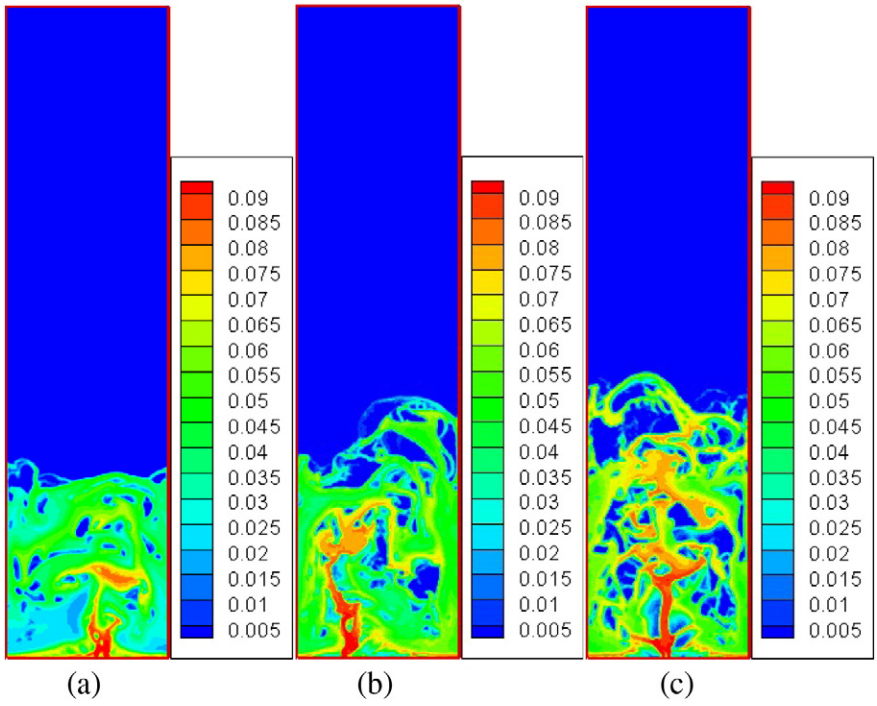

Fig. 9. Methane formation rate ($kg \cdot m^{-3}\ s^{-1}$) in the fluidized bed methanation reactor at 20 s under different inlet superficial gas velocity: (a) $U_f = 0.05$ m/s, (b) $U_f = 0.10$ m/s, and (c) $U_f = 0.15$ m/s.

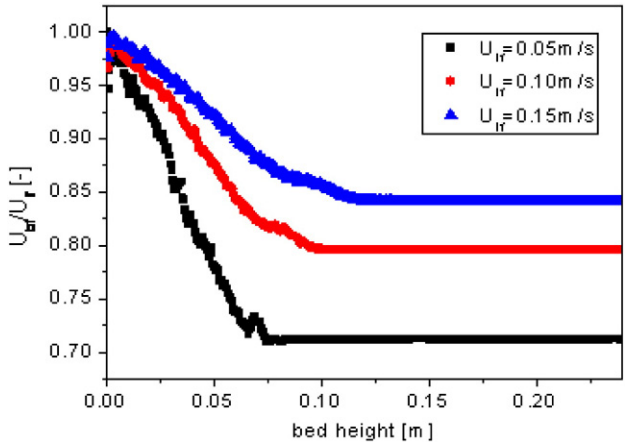

Fig. 10. Time-average superficial gas velocities along the bed height under different gas inlet velocities. Simulations carried out at the same conditions as in Fig. 9.

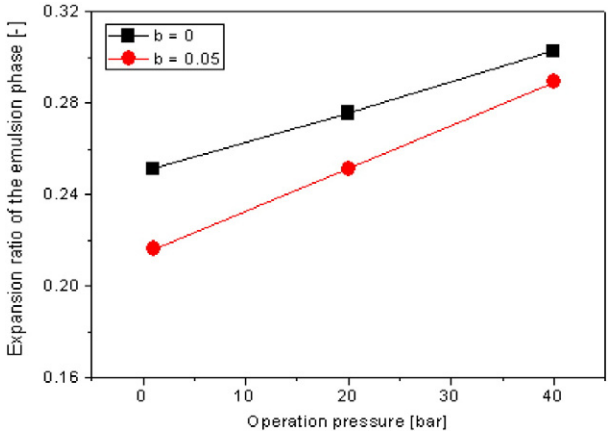

Fig. 12. Effect of pressure on the expansion ratio of the emulsion phase in the methanation fluidized bed reactor (W × H: 0.06 m × 0.24 m). Simulations carried out with a reaction coefficient *b* of 0.05, particle number of 480,000, and inlet gas velocity of 0.10 m/s. Other simulation conditions listed in Table 1.

4.3.4. Effect of bed inventory

The bed aspect ratio has a significant influence on solid mixing [51,52] and gas dispersion [53] in a bubbling fluidized bed, indicating the interaction between of the two phases changing with the amount of bed materials. Hence the interphase mass transfer rate may also change accordingly. Therefore, the links between the expansion of the emulsion phase and bed inventory were also investigated.

Fig. 13 shows the time-averaged expansion ratio of the emulsion phase in the methanation fluidized bed reactor for different bed inventories at a fixed inlet superficial gas velocity of 0.05 m/s. In the absence of the methanation reaction, it can be observed that the expansion ratio of the emulsion phase is shown to decline slightly. When the reaction is turned on, the expansion ratio of the emulsion phase changes from 0.235 to 0.200 by doubling the bed inventory. This is because a larger bed inventory, thus a higher initial bed height, allows longer time for bubbles to grow in the bed [54,55]. Hence, as shown in Fig. 14, bigger bubbles can be detected in the upper part of the reactor at a larger bed inventory. Larger bubble size at the upper part means less gas passing through the emulsion phase and thus smaller voidage in the emulsion phase at the upper part. Concurrently, due to the methanation reaction in the emulsion phase, the gas volumetric flow reduces significantly along the bed height direction. When the reaction kinetics and inlet superficial gas velocity keeps unchanged, more reactant gas is converted in a dense bed as bed height increases. In this case, the gas volumetric flow passing through the emulsion phase becomes even smaller at the upper section. These together make the contraction of the emulsion phase more serve at a larger bed inventory.

Our results also show that the reduction of superficial gas velocity in the dense bed becomes more serious with a larger bed inventory. This result agrees qualitatively with the experimental results in [56], which showed that the degree of *defluidization* increases with initial bed height. We noted that in their experiments, partial *defluidization*

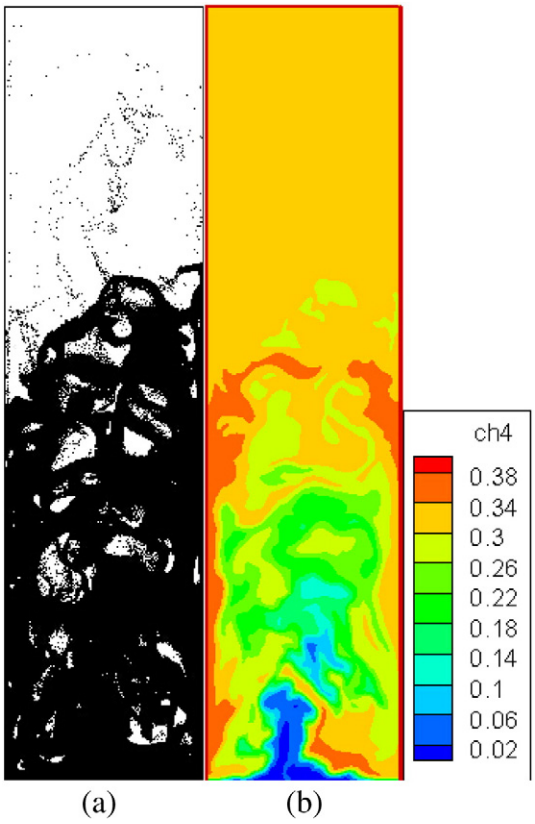

Fig. 11. Flow patterns (a) and the corresponding mass fraction distribution mass fraction of CH_4 (b) in the methanation fluidized bed reactor at 20 s. Simulations carried out with a reaction coefficient *b* of 0.05, particle number of 480,000, gas inlet velocity of 0.10 m/s. and pressure of 40 bar. Other simulation conditions listed in Table 1.

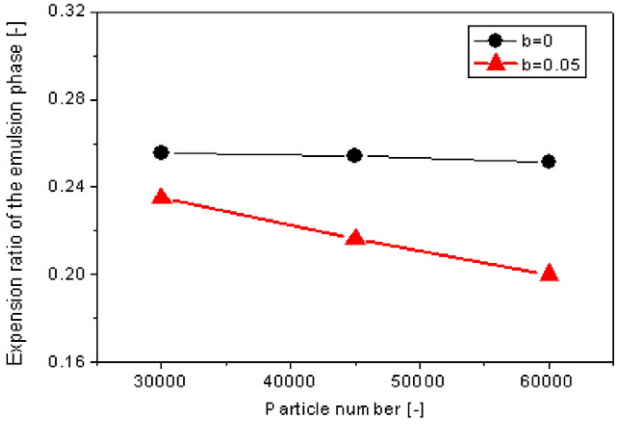

Fig. 13. The expansion ratio of the emulsion phase under different bed inventories in the methanation fluidized bed reactor (W × H: 0.06 m × 0.24 m). Simulations carried out with a reaction coefficient *b* of 0.05, pressure of 1 bar, and inlet superficial gas velocity of 0.05 m/s. Other simulation conditions listed in Table 1.

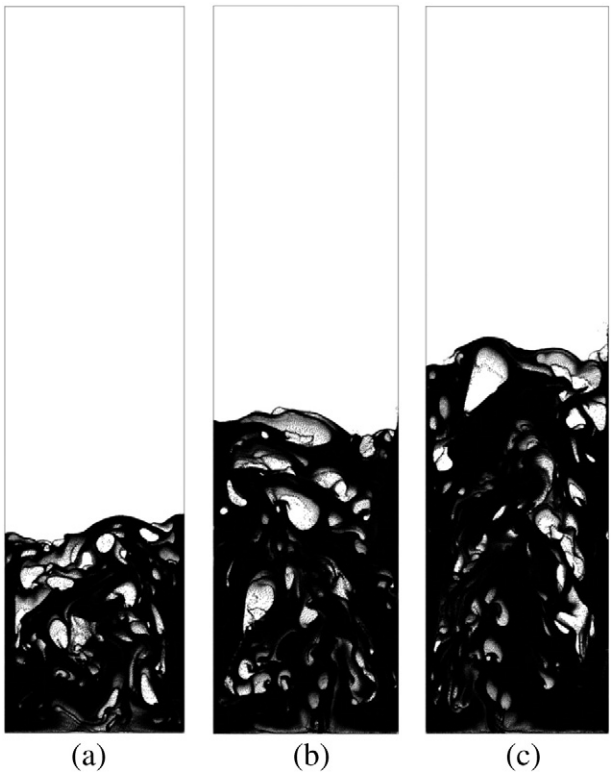

Fig. 14. Snapshots of flow patterns in the fluidized bed methanation reactor (W × H: 0.06 m × 0.24 m) at 20 s under different bed inventories: (a) $N_p = 300{,}000$, (b) $N_p = 480{,}000$, and (c) $N_p = 600{,}000$. Simulations carried out with a reaction coefficient b of 0.05, pressure of 1 bar, and inlet superficial gas velocity of 0.05 m/s. Other simulation conditions listed in Table 1.

phenomenon was detected in a fluidized bed having a much larger height-to-diameter ratio than that in our study. In our study, the direct *defluidization* was not detected but instead the apparent contraction of the emulsion phase was found. This is due to the small fluidized bed employed in our CFD–DEM simulations.

5. Conclusion

In methanation fluidized bed reactors, the gas volumetric flow reduction can cause severe problems for fluidization quality. In extreme cases, unwanted *defluidization* may be observed. In this work, we studied the change of the expansion ratio of the emulsion phase rather than direct prediction of the *defluidization* in methanation fluidized bed reactors by use of a well-proved CFD–DEM code originally developed by Prof. Hans Kuipers' group. The hydrodynamics in the bed, especially the minimum fluidization velocity and bubble dynamics, was first investigated. Then the effects of operation conditions such as reaction rate, superficial gas velocity, pressure, and bed inventory on the expansion ratio of the emulsion phase were studied and discussed.

It was found that traditional correlations cannot be directly used to predict the minimum fluidization velocity (U_{mf}) due to volumetric flow reduction in a dense bed. A much higher minimum fluidization velocity, estimated based on the reactant gas at the inlet, is required to maintain good fluidization quality in the methanation fluidized bed reactor. Fast bubbles were identified in the fluidized beds as Geldart A particles were used as catalyst. The gas circulation around the fast bubbles is found responsible for the worsened gas exchange between gas bubbles and emulsions phase, which results in the apparent contraction of emulsion phase since the gas reduced by methanation reaction in the emulsion phase cannot be completely compensated by gas flowing from bubbles.

The inlet superficial gas velocity has a minor effect on the expansion ratio of the emulsion phase when there is no reaction occurring in the fluidized bed, which agrees well with experimental results by Kai et al. [39]. However, in a methanation fluidized bed reactor, the inlet superficial gas velocity affects the expansion ratio of the emulsion phase in a complicated manner, owning to the larger bubble size and shorter gas residence time in the emulsion phase. In terms of enhanced heat transfer, a higher inlet superficial gas velocity is favored for operating the methanation fluidized bed reactor. Higher pressure is preferred in improving the expansion of emulsion phase since it reduces the bubble size and thus increases the gas flow in the emulsion phase. The enhanced mass transfer between gas bubbles and emulsion phase can be found at a higher pressure. Higher initial bed height was shown to have a negative impact on the expansion ratio of the emulsion phase, and worsen the fluidization quality in general.

The results from this modeling study can help us understand the fluidization behavior in methanation fluidized bed reactors. In our laboratory, a methanation fluidized bed reactor is currently under development. The information obtained from the CFD–DEM simulations is critical for us to optimize the rector design.

Nomenclature

u	velocity, m/s
u_g	gas superficial velocity, m/s
p	gas pressure, Pa
Y_i	mass fraction of species i, dimensionless
S	the source term
M_i	molar mass of gas species, kg/mol
R	rate of methanation (mol/kg$_{cat}$/s)
k	reaction constant (−)
K_i	absorption constant of species i
V_{cell}	the local volume of a computational cell, m^3
H_g	the gas enthalpy
m_e	the effective mass of a linear spring–dashpot system, kg
m_p	mass of particle, kg
V_p	volume of particle, m^3
$\vec{F}_{cont,\,p}$	the contact force acting on the particle, (N)
I_p	the moment of inertia, kg·m^2
Ω_p	the rotational acceleration, r/s^2
ϖ_p	the rotational velocity, r/s

Greek symbols

ε_g	local porosity (−)
δ_e	expansion ratio of the emulsion phase (−)
μ_g	gas viscosity, Pa·s
ρ	density, kg/m^3
β	the momentum transfer coefficient
τ_g	viscous stress tensor
τ	osscilating period of a linear spring–dashpot system

Subscripts and superscripts

e	emulsion or dense phase
mf	minimum fluidization condition
g	gas
p	particle or pressure
b	bed

Acknowledgments

Prof. Hans Kuipers is acknowledged for encouraging us to use the CFD–DEM code developed in his group. The authors are grateful to BP for the financial support of this work via the BP-DICP Energy Innovation Laboratory (EIL) Program. Mao Ye is also supported by the National Natural Science Foundation of China (Grant No. 91334205).

References

[1] J. Kopyscinski, T.J. Schildhauer, S. Biollaz, Production of synthetic natural gas (SNG) from coal and dry biomass—a technology review from 1950 to 2009, Fuel 89 (2010) 1763–1783.
[2] S.V. Ho, P. Harriott, The kinetics of methanation on nickel catalysts, J. Catal. 64 (1980) 272–283.
[3] D.C. Gardner, C.H. Bartholomew, Kinetics of carbon deposition during methanation of carbon monoxide, Ind. Eng. Chem. Prod. Res. Dev. 20 (1981) 80–87.
[4] K. Eisenlohr, F. Moeller, M. Dry, Influence of certain reaction parameters on methanation of coal gas to SNG, Fuels ACS Div Preprints, 19 (1974) 1–9.
[5] H. Topsøe, From Solid Fuels to Substitute Natural Gas (SNG) Using TREMP, 2009, http://www.topsoe.com.
[6] R. Ensell, H. Stroud, The British gas HICOM methanation process for SNG production, The 1983 International Gas Research Conference, British Gas Corporation, UK, 1983.
[7] M. Seemann, T. Schildhauer, S. Biollaz, S. Stucki, A. Wokaun, The regenerative effect of catalyst fluidization under methanation conditions, Appl. Catal. A Gen. 313 (2006) 14–21.
[8] G. White, T. Roszkowski, D. Stanbridge, Predict carbon formation. Synthesis gas and SNG operations, Hydrocarb. Process. 54 (1975) 375–382.
[9] T. Kai, Y. Shirakawa, T. Takahashi, S. Furusaki, Change in bubble behavior for different fluidizing gases in a fluidized bed, Powder Technol. 51 (1987) 267–271.
[10] T. Kai, M. Murakami, K. Yamasaki, T. Takahashi, Relationship between apparent bed viscosity and fluidization quality in a fluidized bed with fine particles, J. Chem. Eng. Jpn. 24 (1991) 494–500.
[11] T. Kai, S. Furusaki, Methanation of carbon dioxide and fluidization quality in a fluid bed reactor—the influence of a decrease in gas volume, Chem. Eng. Sci. 42 (1987) 335–339.
[12] T. Kai, K. Toriyama, K. Nishie, T. Takahashi, M. Nakajima, Effect of volume decrease on fluidization quality of fluidized catalyst beds, AIChE J. 52 (2006) 3210–3215.
[13] T. Li, C. Guenther, MFIX–DEM simulations of change of volumetric flow in fluidized beds due to chemical reactions, Powder Technol. 220 (2012) 70–78.
[14] C. Wu, D. Tian, Y. Cheng, CFD-DEM simulation of syngas-to-methane process in a fluidized-bed reactor, in: S.D. Kim, Y. Kang, J.K. Lee, Y.C. Seo (Eds.),The 13th International Conference on Fluidization—New Paradigm in Fluidization Engineering, Gyeong-ju, Korea 2010, 733-740 ECI Symposium Series, 2010, pp. 733–740.
[15] Y. Chu, B. Chu, X. Wei, Q. Zhang, F. Wei, An emulsion phase condensation model to describe the defluidization behavior for reactions involving gas–volume reduction, Chem. Eng. J. 198 (2012) 364–370.
[16] Y. Liu, O. Hinrichsen, CFD simulation of hydrodynamics and methanation reactions in a fluidized-bed reactor for the production of synthetic natural gas, Ind. Eng. Chem. Res. 53 (2014) 9348–9356.
[17] Y. Zhang, Y. Zhao, M. Ye, R. Xiao, Z. LiuA, DEM study of the reduction of volumetric flow in bubbling fluidized bed methanation reactors, in: J.A.M. Kuipers, R.F. Mudde, J.R. van Ommen, N.G. Deen (Eds.), The 14th International Conference on Fluidization—From Fundamentals to Products, Noordwijkerhout, the Netherlands, 2013 ECI Symposium Series, 2013, pp. 87–94.
[18] T. Kai, S. Furusaki, Effects of gas properties on the behaviour of fluidized beds of small particles, J. Chem. Eng. Jpn. 19 (1986) 67–71.
[19] H. Zhu, Z. Zhou, R. Yang, A. Yu, Discrete particle simulation of particulate systems: a review of major applications and findings, Chem. Eng. Sci. 63 (2008) 5728–5770.
[20] B. Hoomans, J. Kuipers, W. Briels, W. Van Swaaij, Discrete particle simulation of bubble and slug formation in a two-dimensional gas-fluidised bed: a hard-sphere approach, Chem. Eng. Sci. 51 (1996) 99–118.
[21] M. Ye, M. Van der Hoef, J. Kuipers, A numerical study of fluidization behavior of Geldart A particles using a discrete particle model, Powder Technol. 139 (2004) 129–139.
[22] N. Deen, M. Van Sint Annaland, M. Van der Hoef, J. Kuipers, Review of discrete particle modeling of fluidized beds, Chem. Eng. Sci. 62 (2007) 28–44.
[23] M. Ye, M. Van der Hoef, J. Kuipers, The effects of particle and gas properties on the fluidization of Geldart A particles, Chem. Eng. Sci. 60 (2005) 4567–4580.
[24] J. Kuipers, K. Van Duin, F. Van Beckum, W. Van Swaaij, A numerical model of gas-fluidized beds, Chem. Eng. Sci. 47 (1992) 1913–1924.
[25] R.J. Hill, D.L. Koch, A.J. Ladd, The first effects of fluid inertia on flows in ordered and random arrays of spheres, J. Fluid Mech. 448 (2001) 213–241.
[26] C. Wu, Y. Cheng, Y. Ding, Y. Jin, CFD–DEM simulation of gas–solid reacting flows in fluid catalytic cracking (FCC) process, Chem. Eng. Sci. 65 (2010) 542–549.
[27] W.L. Vargas, J. McCarthy, Heat conduction in granular materials, AICHE J. 47 (2001) 1052–1059.
[28] W. Ranz, Friction and transfer coefficients for single particles and packed beds, Chem. Eng. Prog. 48 (1952) 247–253.
[29] P.A. Cundall, O.D.L. Strack, A discrete numerical model for granular assemblies, Geotechnique (1979) 47–65.
[30] Y. Tsuji, T. Kawaguchi, T. Tanaka, Discrete particle simulation of two-dimensional fluidized bed, Powder Technol. 77 (1993) 79–87.
[31] J. Kopyscinski, T.J. Schildhauer, S.M. Biollaz, Fluidized-bed methanation: interaction between kinetics and mass transfer, Ind. Eng. Chem. Res. 50 (2010) 2781–2790.
[32] C. Wen, Y.H. Yu, Mechanics of fluidization, AIChE Symp. Ser. 62 (1966) 100–111.
[33] T. Kai, K. Toriyama, T. Takahashi, M. Nakajima, Fluidization quality of fluidized catalyst beds involving a decrease in gas volume, Stud. Surf. Sci. Catal. 159 (2006) 497–500.
[34] W.-C. Yang, Handbook of Fluidization and Fluid–Particle Systems, Marcel Dekker, New York, 2003.
[35] T. Kai, A. Matsumura, K. Sezutsu, T. Nakazato, M. Nakajima, Gas recycling in fluidized bed to avoid defluidization for reactions accompanied by decrease in the number of moles, Chem. Eng. J. 215–216 (2013) 671–677.
[36] A. Weimer, G. Quarderer, On dense phase voidage and bubble size in high pressure fluidized beds of fine powders, AICHE J. 31 (1985) 1019–1028.
[37] V.G. Kul'bachnyi, K.E. Makhorin, Pressure distribution around a single bubble moving in a fluidized bed, J. Eng. Phys. 21 (1971) 1493–1497.
[38] S. Karimipour, T. Pugsley, A critical evaluation of literature correlations for predicting bubble size and velocity in gas–solid fluidized beds, Powder Technol. 205 (2011) 1–14.
[39] T. Kai, T. Imamura, T. Takahashi, Hydrodynamic influences on mass transfer between bubble and emulsion phases in a fine particle fluidized bed, Powder Technol. 83 (1995) 105–110.
[40] C. Chavarie, J. Grace, Interphase mass transfer in a gas fluidized bed, Chem. Eng. Sci. 31 (1976) 741–749.
[41] L. Huilin, Z. Yunhua, J. Ding, D. Gidaspow, L. Wei, Investigation of mixing/segregation of mixture particles in gas–solid fluidized beds, Chem. Eng. Sci. 62 (2007) 301–317.
[42] S. Limtrakul, A. Chalermwattanatai, K. Unggurawirote, Y. Tsuji, T. Kawaguchi, W. Tanthapanichakoon, Discrete particle simulation of solids motion in a gas–solid fluidized bed, Chem. Eng. Sci. 58 (2003) 915–921.
[43] S. Limtrakul, J. Chen, P.A. Ramachandran, M.P. Duduković, Solids motion and holdup profiles in liquid fluidized beds, Chem. Eng. Sci. 60 (2005) 1889–1900.
[44] S. Karimi, Z. Mansourpour, N. Mostoufi, R. Sotudeh-Gharebagh, CFD–DEM study of temperature and concentration distribution in a polyethylene fluidized bed reactor, Part. Sci. Technol. 29 (2011) 163–178.
[45] J. Field, J. Demeter, A. Forney, D. Bienstock, Development of catalysts and reactor systems for methanation, Ind. Eng. Chem. Prod. Res. Dev. 3 (1964) 150–153.
[46] R.C. Streeter, Recent developments in fluidized-bed methanation research, The 9th Synthetic Pipeline Gas Symposium, Chicago, IL, 1977.
[47] J. Yates, Effects of temperature and pressure on gas–solid fluidization, Chem. Eng. Sci. 51 (1996) 167–205.
[48] G. Barreto, J. Yates, P. Rowe, The effect of pressure on the flow of gas in fluidized beds of fine particles, Chem. Eng. Sci. 38 (1983) 1935–1945.
[49] J. de Carvalho, Dense phase expansion in fluidised beds of fine particles: the effect of pressure on bubble stability, Chem. Eng. Sci. 36 (1981) 413–416.
[50] H. Piepers, E.J.E. Cottaar, A. Verkooijen, K. Rietema, Effects of pressure and type of gas on particle–particle interaction and the consequences for gas–solid fluidization behaviour, Powder Technol. 37 (1984) 55–70.
[51] H. Tanfara, T. Pugsley, C. Winters, Effect of particle size distribution on local voidage in a bench-scale conical fluidized bed dryer, Dry. Technol. 20 (2002) 1273–1289.
[52] H. Norouzi, N. Mostoufi, Z. Mansourpour, R. Sotudeh-Gharebagh, J. Chaouki, Characterization of solids mixing patterns in bubbling fluidized beds, Chem. Eng. Res. Des. 89 (2011) 817–826.
[53] H.I. Cho, C.H. Chung, G.Y. Han, G.R. Ahn, J.S. Kong, Axial gas dispersion in a fluidized bed of polyethylene particles, Korean J. Chem. Eng. 17 (2000) 292–298.
[54] P. Rowe, C. Yacono, The bubbling behaviour of fine powders when fluidised, Chem. Eng. Sci. 31 (1976) 1179–1192.
[55] D. Geldart, The effect of particle size and size distribution on the behaviour of gas-fluidised beds, Powder Technol. 6 (1972) 201–215.
[56] T. Kai, M. Furukawa, T. Nakazato, M. Nakajima, Prevention of defluidization by gas dilution for reactions involving gas–volume reduction, Chem. Eng. J. 166 (2011) 1126–1131.